D.P. Landau S.P. Lewis H.-B. Schüttler
(Eds.)

Computer Simulation Studies in Condensed-Matter Physics XVI

Proceedings of the Fifteenth Workshop
Athens, GA, USA, February 24–28, 2003

With 110 Figures

Springer

Professor David P. Landau, Ph.D.
Professor Steven P. Lewis, Ph.D.
Professor Heinz-Bernd Schüttler, Ph.D.
Center for Simulational Physics
The University of Georgia
Athens, GA 30602-2451, USA

ISSN 0930-8989

ISBN 3-540-20021-5 Springer-Verlag Berlin Heidelberg New York

Bibliographic information published by Die Deutsche Bibliothek
Die Deutsche Bibliothek lists this publication in the Deutsche Nationalbibliografie; detailed bibliographic data is available in the Internet at <http://dnb.ddb.de>.

Springer is a part of Springer Science+Business Media.

springeronline.com

Printed in Germany

Typesetting by the authors/editors
Cover concept: eStudio Calamar Steinen
Cover production: *design & production* GmbH, Heidelberg

Printed on acid-free paper SPIN: 10958070 57/3141/ad 5 4 3 2 1 0

31 Molecular Dynamics Simulation of Nanoindentation

K. Michielsen, M.T. Figge, H. De Raedt, and J.T.M. De Hosson

University of Groningen, Materials Science Centre,
Department of Applied Physics,
Nijenborgh 4, NL-9747 AG, Groningen, The Netherlands
E-mail: kristel@phys.rug.nl, URL: http://www.compphys.org

Abstract. Molecular dynamics simulations are used to investigate the nucleation and dynamics of dislocations during nanoindentation of a (111) FCC plane. The core structure around the dislocation is visualized by coloring the atoms with deviating coordination number and its Burgers vector is automatically determined. Discontinuities in the load-depth curves are related to the nucleation of edge dislocation dipoles (loading) and the annihilation of dislocations (unloading).

31.1 Introduction

In nanoindentation experiments an indenter with a contact area on a nanoscale is pushed at constant speed v from a given height h_b to a given depth h_e into the material (loading), and is subsequently retracted to its original position following the same trajectory as for the loading process (unloading). For single crystals the measured load-displacement response, which shows the force required to push the tip a certain distance into the material, shows characteristic discontinuities.

It has been shown that molecular dynamics (MD) simulations can provide a qualitative analysis of discrete plasticity events that are consistent with experimental observations of nanoindentation in single crystals [1]. In MD simulations several methods are used to identify the location and type of defects in the material. Amongst others, these techniques rely on the selection of atoms on the basis of their potential energy, their centrosymmetry parameter [2], their coordination number, their atomic stress tensor or their slip vector [3]. Recently, the Λ-criterion has been used in MD simulations to predict the location and slip character (slip plane and Burgers vector) of a homogeneously nucleated defect [1]. Below we present a technique to automatically determine the Burgers vector in MD simulations of nanoindentation of a crystal plane.

31.2 Model and Simulation Method

The system we study is the (111) plane of an FCC lattice consisting of N atoms with mass m. Prior to indentation the system is defect-free. The width

Springer Proceedings in Physics, Volume 95
Computer Simulation Studies in Condensed-Matter Physics XVI
Eds.: D.P. Landau, S.P. Lewis and H.-B. Schüttler

of the system is given by $L_x = xa_0$ and the thickness or height by $L_y = ya_0$, where $a_0 = a/\sqrt{2}$ and a denotes the lattice parameter. The atoms at the bottom layer and at the left and right boundary of the material are kept fixed. Thus, we do not use periodic boundary conditions.

Since our goal is to study generic material properties and dislocation nucleation and dynamics during indentation we consider a simple non-trivial model. We assume that the interatomic forces are described by a Lennard-Jones (LJ) potential $V(r_{ij}) = 4\epsilon\left[(\sigma/r_{ij})^{12} - (\sigma/r_{ij})^{6}\right]$, where r_{ij} denotes the distance between atoms i and j, ϵ denotes the minimum of the potential function and σ denotes the interatomic distance at which the potential is zero. The potential quickly falls to negligible values for large values of r_{ij}. Hence in practice a truncation r_c can be applied beyond which the force between particles is defined to vanish [4]. A typical cutoff distance is $r_c = 2.5\sigma$ [4]. However for zero-temperature, harmonic theory shows that in order to recover the correct elastic continuum theory, the radius r_c has to be increased to at least 3.5σ.

In this study we use a rigid half-sphere tip with diameter $d_t = da_0$. Only the outer atoms of the tip interact with the dynamic material atoms. The interaction is considered to be purely repulsive and modeled by the repulsive part of the LJ potential. As such, there is zero friction between the indenter and the material. The potential parameters are denoted by σ' and ϵ'. The direction of indentation is $[\bar{1}2\bar{1}]$. The indenter moves towards the material with increments of y_t over N_t time steps Δt, corresponding to an indentation speed $v = y_t/\Delta t N_t$. Prior to indentation the topmost layer of the material is positioned at $y = 0$, hence $h_b > 0$ and $h_e < 0$. The force acting on the indenter is calculated by summing the y-components of forces acting on the individual outer atoms of the tip.

We use standard MD technology [4] to simulate the motion of the material atoms. Equations of motion are integrated using the Verlet and a fourth-order simplectic integrator [5]. We divide the simulation space into small cubic cells with dimensions $R_c > r_c$. Each cell is represented by a linked-list of the atoms within it [4].

The use of some kind of thermostat is mandatory to dissipate the energy that is added to the system by pressing the indenter into the material. We have studied various mechanisms: Nosé–Hoover thermostat [6], Langevin dynamics [7] and the Berendsen thermostat [8]. Our test shows that the Berendsen thermostat dissipates the extra energy very fast. The Berendsen thermostat does not exactly reproduce the canonical distribution but is widely used because of its stability and efficiency in MD simulations [9]. Moreover also the more "rigorous" Nosé–Hoover thermostat can fail to reproduce the expected statistical mechanical behavior [9]. Since we are interested in the mechanism of defect nucleation under nanoindentation, a non-equilibrium process, and the analysis of the emerging dislocations, the use of the Berendsen thermostat is justified. We use the kinetic energy to define the effective temperature T.

31.3 Dislocation Analysis

Defects in the material are visualized by coloring the atoms according to their coordination number C. The coordination number counts the number of nearest neighbors of an atom. In a static and perfect (111) plane of a FCC lattice, C counts all atoms at a distance $D = a_0$ of the atom under consideration. Hence, all atoms have $C = 6$. In our MD simulations the atoms are not static and therefore we take $D = 3a_0/2$ to compute C. So-called "defect atoms" and atoms at the system boundaries have $C \neq 6$.

We calculate C for each atom and subsequently group the defect atoms in "defects" by searching for nearest-neighbor defect atoms of the defect atom under consideration. In this way we label the defects consisting of connected defect atoms.

For each defect we mark the nearest-neighbor atoms of the defect atoms which are not belonging to the defect itself, i.e. we mark the atoms forming the outer perimeter of the defect (see the encircled atoms surrounding the defects in Fig. 31.3). These atoms form a closed loop enclosing the dislocation line. We use this circuit of atoms to compute the Burgers vector. We move from one atom in the loop to the next and determine the vector between them. We compare this vector with the perfect FCC lattice vectors and store the lattice vector which resembles the vector between the atoms the most. We then take the next atom in the loop, repeat the above procedure and add the newly determined lattice vector to the previous one. We continue until the loop closes. The resulting vector from summing up the lattice vectors is the Burgers vector $\boldsymbol{b}$. The sense of $\boldsymbol{b}$ is chosen such that the Burgers vector points from the end-to-the-beginning of the circuit (in the sense of a right-handed screw) in the perfect crystal [10].

31.4 Results

We report on nanoindentation simulations for two systems of different size, referred to as system 1 and 2, respectively. System 1 (2) contains $N = 5075(20549)$ atoms, $L_x = 99a_0(199a_0)$ and $L_y = 25a_0(51a_0)$, where $a_0 = 0.16837\,\text{nm}$. Hence the system has a thickness of 7.3 nm (14.9 nm) and a length of 16.7 nm (33.5 nm). The other simulation parameters are given in the table in Fig. 31.3.

We first indent the defect-free system 1. The initial deformation of the material is elastic but at a certain indentation depth two subsurface edge dislocation dipoles nucleate slightly displaced from the loading axis. The dipoles split: One dislocation proceeds towards the material surface and forms a surface slip step of one atomic diameter, a second dislocation proceeds into the material. The two dislocations of opposite sense that migrate into the material (denoted by 1 and 2 in Figs. 31.3 and 31.3) subsequently glide in opposite $\langle 110 \rangle$ slip directions. The Burgers vector of dislocation 1 is $\boldsymbol{b}_1 = [0\bar{1}1]/2$ and

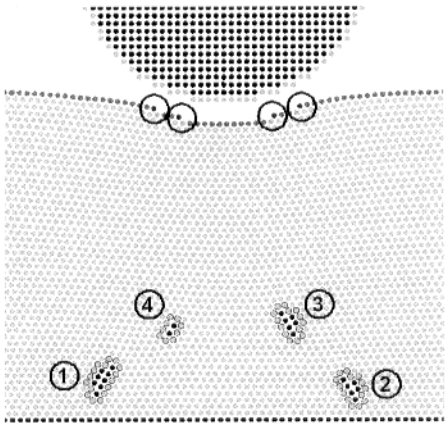

Model parameters
$m = 9.298810^{-26}$kg
$\epsilon = 1$eV
$\sigma = 0.15$nm
$T = 50$ K
$R_c = 1.5$ nm
$\Delta t = 2.5$ fs
$d_t = 6.7$ nm
$\epsilon' = 10$ eV
$\sigma' = 0.4$ nm
$y_t = 0.01$ nm
$N_t = 800$
$v = 5$ m/s
$h_b = 1$ nm
$h_c = -0.5$ nm

Fig. 31.1. Left: MD simulation of system 1 after four dipole nucleation events, illustrating the formation of four surface slip steps of one atomic diameter (encircled at the surface of the material) and four edge dislocations (indicated by 1, 2, 3 and 4) confined within the material. The atoms are colored according to their coordination number. Right: Simulation parameters

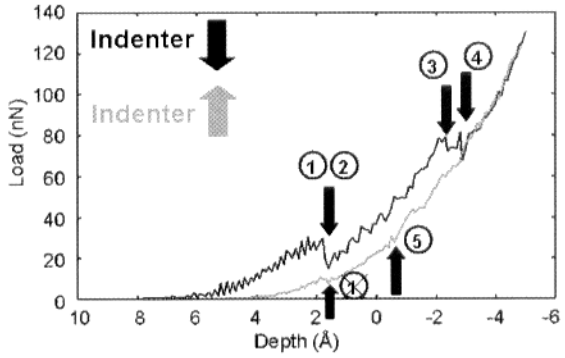

Fig. 31.2. Load-indentation depth response of system 1 during loading (black) and unloading (grey). The discontinuities in the loading curve correspond to the nucleation of dislocation dipoles, indicated by 1, 2, 3 and 4 corresponding to the edge dislocations migrating into the material (see Fig. 31.3). The small drops in the unloading curve correspond to the annihilation of dislocations, indicated by 5 and the traversed 1

of dislocation 2, $\boldsymbol{b}_2 = [\bar{1}10]/2$. Upon further loading the atoms in a small localized region under the slip steps become disordered but no dislocations are nucleated at the slip steps. Instead, a third and fourth subsurface edge dislocation dipole is nucleated. Again two dislocations move towards the ma-

terial surface to create surface slip steps and two other dislocations (denoted by 3 and 4 in Figs. 31.3 and 31.3) with Burgers vectors $\boldsymbol{b}_3 = [0\bar{1}1]/2$ and $\boldsymbol{b}_4 = [\bar{1}10]/2$ migrate into the material. The depth of nucleation is increased with respect to the first subsurface dipole nucleation events. Since the slip plane orientation is always 30° off axis, the slip steps appear at increasing distances from the loading axis. This process of subsequent subsurface nucleation events was also observed in monotonic loading experiments of the Bragg-Nye bubble raft [11]. During the unloading process dislocations 3 and 4 move towards each other along their slip directions, collide and form a new edge dislocation (denoted by 5 in Fig. 31.3) that subsequently glides in the horizontal $\langle 101 \rangle$ direction. The Burgers vector of dislocation 5 is $\boldsymbol{b}_5 = \boldsymbol{b}_3 + \boldsymbol{b}_4 = [101]/2$. Upon further unloading, dislocation 1 migrates to the material surface and disappears thereby creating an extra surface slip step. In the final stage the material has an imprint of the indenter remaining on its surface. Five surface slip steps of one atomic diameter are created on the surface of the material and two edge dislocations remain as defects inside the material.

Figure 31.3 shows the load-depth response of the system. It is seen that each significant discontinuous load relaxation corresponds with the nucleation of an edge dislocation dipole. This was also seen in [1]. Although less clearly visible, the annihilation of dislocations gives rise to discontinuities in the unloading curve.

Indentation of system 2 shows similar results (not shown). In this system only three subsurface edge dislocation dipoles are nucleated. Upon unloading the third dislocation, that has migrated into the material, moves to the surface, disappears and removes one surface slip step. The fact that there are less dislocations nucleated can be understood from the fact that this system is much larger compared to system 1 and hence less stress is build up in the system. The load-depth response of system 2 shows similar behavior as that of system 1 but the applied loads are a factor of two smaller compared to those in system 1.

In summary, relatively small MD systems are sufficient to investigate the qualitative behavior of dislocation nucleation and annihilation in nanoindentation experiments. This observation may be important for the coupling of atomistic simulations to continuum dynamics [12].

Acknowledgement

This work is partially supported by the "Stichting Nationale Computer Faciliteiten (NCF)" and the "Nederlandse Organisatie voor Wetenschappelijk Onderzoek
(NWO)".

References

1. J. Li, K.J. Van Vliet, T. Zhu, S. Yip, S. Suresh: Nature **418**, 307 (2002)
2. C.L. Kelchner, S.J. Plimpton, J.C. Hamilton: Phys. Rev. B **58**, 11085 (1998)
3. J.A. Zimmerman, C.L. Kelchner, P.A. Klein, J.C. Hamilton, S.M. Foiles: Phys. Rev. Lett. **87**, 165507 (2001)
4. D.C. Rapaport: *The Art of Molecular Dynamics Simulation.* (Cambridge University Press, Cambridge 2001)
5. M. Suzuki: J. Math. Phys. **26**, 601 (1985)
6. S. Nosé: Mol. Phys. **52**, 255 (1984); W.G. Hoover: Phys. Rev. A **31**, 1695 (1985)
7. G.S. Grest and K. Kremer: Phys. Rev. A **33**, 3628 (1986)
8. H.J.C. Berendsen, J.P.M. Postma, W.F. van Gunsteren, A. DiNola and J.R. Haak: J. Chem. Phys. **81**, 3684 (1984)
9. M. D'Alessandro, A. Tenenbaum, A. Amadei: J. Phys. Chem. B **106**, 5050 (2002)
10. B.A. Bilby, R. Bullough and E. Smith: Proc. Roy. Soc. A **231**, 263 (1955)
11. K.J. Van Vliet, S. Suresh: Philos. Mag. A **82**, 1993 (2002)
12. L.E. Shilkrot, W.A. Curtin, R.E. Miller: J. Mech. Phys. Solids **50**, 2085 (2002)